

Journal of Biomedical Optics

SPIEDigitalLibrary.org/jbo

Optimizing *in vivo* small animal Cerenkov luminescence imaging

Antonello E. Spinelli
Federico Boschi



SPIE

Optimizing *in vivo* small animal Cerenkov luminescence imaging

Antonello E. Spinelli^a and Federico Boschi^b

^aSan Raffaele Scientific Institute, Medical Physics Department, Milan, Italy

^bUniversity of Verona, Department of Neurological, Neuropsychological, Morphological and Motor Sciences, 37134 Verona, Italy

Abstract. *In vivo* Cerenkov luminescence imaging is a rapidly growing molecular imaging research field based on the detection of Cerenkov radiation induced by beta particles when traveling through biological tissues. We investigated theoretically the possibility of enhancing the number of the detected Cerenkov photons in the near infrared (NIR) region of the spectrum. The analysis is based on applying a photon propagation diffusion model to Cerenkov photons in the tissue. Results show that despite the smaller number of Cerenkov photons in the NIR region, the fraction exiting the tissues is greater than in the visible range, and thus, a charge-coupled device detector optimized for the NIR range will allow to obtain a higher signal. The comparison was performed considering Cerenkov point sources located at different depths inside the animal. We concluded that the improvement can be up to 35% and is more significant when the Cerenkov source to be imaged is located deeper inside the animal. © 2012 Society of Photo-Optical Instrumentation Engineers (SPIE). [DOI: 10.1117/1.JBO.17.4.040506]

Keywords: charge-coupled-device imagers; image acquisition; recording imaging.

Paper 12047L received Jan. 23, 2012; revised manuscript received Feb. 22, 2012; accepted for publication Feb. 28, 2012; published online Apr. 23, 2012; corrected Apr. 25, 2012.

In vivo Cerenkov luminescence imaging (CLI) is a rapidly growing molecular imaging research field based on the detection of Cerenkov radiation induced by beta particles when traveling through biological tissue with a velocity greater than the speed of light in the tissue. In the past two years several papers have been published investigating the use of Cerenkov radiation to image different radiotracers,¹⁻⁷ as an excitation source for quantum dots,⁸⁻¹⁰ and as a light source for phototherapy.¹¹

A useful extension of planar CLI was recently obtained by introducing Cerenkov luminescence tomography (CLT) using finite element methods^{12,13} or multispectral approaches.¹⁴

Generally speaking, all these studies pay little or no attention to exploiting the peculiar properties of the Cerenkov light spectrum. For example, in our previous work^{2,4} the shape of the Cerenkov spectrum has been used to obtain, respectively, the source depth or to reconstruct 3-D images using a multispectral approach.¹⁴

It is well known that the number of the emitted Cerenkov photons per unit of wavelength λ shows a $1/\lambda^2$ dependence,¹⁵ and thus a larger number of photons are emitted at shorter wavelengths and vice versa. This property was used by Ref. 16 to investigate theoretically the possible use of fiber probes for brain mapping in order to avoid the typical absorption of the short wavelength part of the spectrum in the biological tissues. Their theoretical analysis showed that the use of fiber probes can significantly increase by three orders of magnitude the detected Cerenkov signal.

However there are some drawbacks of using an approach based on fiber probes, such as its invasiveness and the fact that it is also not possible to obtain continuous images of the Cerenkov sources as in CLI or CLT.

In this work we propose a quite opposite and, to some extent, counterintuitive approach to enhance the number of the detected Cerenkov photons. More precisely, our main goal was to investigate the detection of Cerenkov photons in the near infrared (NIR) region of the spectrum where the tissues show a smaller absorption coefficient.

In the rest of this short communication we will present a theoretical analysis based on applying a photon propagation diffusion model to Cerenkov photons in the tissue. The detection of the photons exiting the tissue will then be simulated considering charge-coupled device (CCD) detectors optimized, respectively, for the visible and NIR spectral regions.

We will show that despite the smaller number of Cerenkov photons in the NIR, the fraction exiting the tissues is greater than in the visible range, and thus, the use of a CCD detector optimized for the NIR range will allow for improvement of the signal.

The photons propagation model used in this work was developed by Haskell and colleagues¹⁷ and applied to preclinical small animal optical imaging by Rice and collaborators.¹⁸ The photon transport in a turbid medium with an absorption coefficient μ_a can be described by the diffusion equation

$$D\nabla^2\phi(\mathbf{r}, t) - \mu_a\phi(\mathbf{r}, t) = \frac{1}{c} \frac{\partial\phi(\mathbf{r}, t)}{\partial t} - S(\mathbf{r}, t), \quad (1)$$

where c is the speed of light, and $\phi(\mathbf{r}, t)$ and $S(\mathbf{r}, t)$ are, respectively, the photon fluence and the source term at position \mathbf{r} and time t . The diffusion coefficient D is equal to

$$D = \frac{1}{3(\mu'_s + \mu_a)}, \quad (2)$$

where μ'_s is the reduced scattering coefficient.

Since we are interested in a noninvasive imaging approach, we assumed that the detector is located outside the tissue and, thus, the whole system geometry can be approximated as a planar semi-infinite medium.

This assumption is more valid for small animal optical systems where the animals are squeezed by two slabs of transparent material.

The semi-infinite medium boundary condition can be included in solving the diffusion equation and for a point source in the case of a detector placed above the medium, the surface radiance L at the tissue surface is equal to

Address all correspondence to: Antonello E. Spinelli, San Raffaele Scientific Institute, Medical Physics Department, Milan, Italy. Tel: +0226432278; E-mail: spinelli.antonello@hsr.it

$$L = \frac{1}{4\pi} \left(\frac{P}{4\pi D} \right) \left\{ \frac{e^{-\mu_{\text{eff}} r_1}}{r_1} - \frac{e^{-\mu_{\text{eff}} r_2}}{r_2} + 3D \left[\frac{d}{r_1^2} \left(\mu_{\text{eff}} + \frac{1}{r_1} \right) e^{-\mu_{\text{eff}} r_1} + \frac{d + 2z_b}{r_2^2} \left(\mu_{\text{eff}} + \frac{1}{r_2} \right) e^{-\mu_{\text{eff}} r_2} \right] \right\}, \quad (3)$$

where P is the source power and the other terms are equal to

$$\mu_{\text{eff}} = \sqrt{3\mu_a(\mu'_s + \mu_a)}, \quad (4)$$

$$z_b = \frac{1 + R_{\text{eff}}}{1 - R_{\text{eff}}} \frac{2}{3(\mu'_s + \mu_a)}, \quad (5)$$

$$r_1 = \sqrt{d^2 + \rho^2}, \quad (6)$$

$$r_2 = \sqrt{(d + 2z_b)^2 + \rho^2}. \quad (7)$$

The terms d and ρ are, respectively, the depth and radiance distance from the detector axis of the point source. For biological tissues with a refractive index n equal to 1.33, the value of the effective reflection coefficient R_{eff} averaged over all angles of incidence at the boundary is equal to 0.431.

At this point it may be useful to remember that the emission of Cerenkov radiation with a radial frequency ω takes place when the ratio between the particle velocity v and the speed of light c is

$$\beta = \frac{v}{c} > \frac{1}{n}. \quad (8)$$

By using the Frank and Tamm theory^{15,19} one can obtain the total energy W emitted by an electron with charge e travelling a short length l in a medium as

$$W = \frac{e^2 l}{c^2} \int_{\beta n > 1} \omega \left(1 - \frac{1}{\beta^2 n^2} \right) d\omega. \quad (9)$$

The corresponding emitted power P_{cer} is thus equal to

$$P_{\text{cer}} = \frac{e^2 \beta}{c} \int_{\beta n > 1} \omega \left(1 - \frac{1}{\beta^2 n^2} \right) d\omega. \quad (10)$$

Equation (10) can be combined with Eq. (3) in order to estimate the power of Cerenkov radiation emitted by a beta particle traveling in the tissues.

The model described above relies on the assumption that the velocity of the beta particle is almost constant along l and, at the same time, such distance needs to be small since Eq. (3) strictly speaking is valid for a point source.

It is useful to remind here that CLI imaging is based on beta emitters used in nuclear medicine these radioisotopes have an endpoint energy typically below 2 MeV, and thus the particles travel a relatively short distance in the medium. More precisely, a recent paper²⁰ based on Monte Carlo simulation showed that

the Cerenkov light production is confined to 2 mm (root mean squared) even for the isotopes with high endpoint energies. For the widely used ¹⁸F the Cerenkov light production take place only within 0.3 mm of the positron path.

In Ref. 18 are presented the full width half maximum (FWHM) values for a point source located at different depths; these FWHM values are generally greater with respect to the distance where Cerenkov light production take places. Therefore for our purposes we can consider the Cerenkov source to be almost equivalent to a point-like source.

The measured radiance L_{meas} will be dependent on the quantum efficiency Q_e of the detector, more precisely

$$L_{\text{meas}}(\lambda) = L(\lambda)Q_e(\lambda). \quad (11)$$

Whereas in this case the dependence by the wavelength λ has been explicitly included in the equation, the wavelength dependence of the tissue μ_{eff} was also taken into account in order to estimate the surface radiance. The values of μ_{eff} at different wavelengths were obtained considering the optical properties of mouse muscle.^{21,22}

In order to investigate the differences in the measured radiance, the Q_e profiles of two different commercial CCD were included in Eq. (11).

In order to compare the detected signals, a figure of merit F was calculated as

$$F = \frac{\int L(\lambda)Q_{\text{NIR}}(\lambda)d\lambda - \int L(\lambda)Q_{\text{VIS}}(\lambda)d\lambda}{\int L(\lambda)Q_{\text{VIS}}(\lambda)d\lambda}, \quad (12)$$

where Q_{VIS} and Q_{NIR} are the quantum efficiencies of two commercial high-quality back-thinned back-illuminated CCD detectors optimized, respectively, for the visible and NIR range.^{23,24}

As an example, the spectrums of the detected Cerenkov light emitted from a point source located at 3-mm depth is shown in Fig. 1. The three plots were obtained by considering an ideal detector having $Q_e = 1$ across the entire spectrum, and the two Q_e values presented in Refs. 23, 24. As one can see by

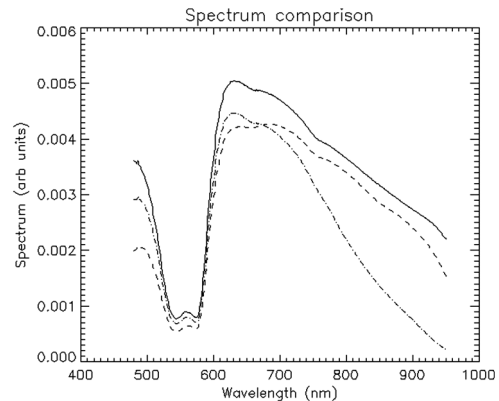


Fig. 1 The plots show the spectrums of the detected Cerenkov light emitted from a point source located at 3-mm depth. The graphs were obtained by considering an ideal detector (continuous line) and the Q_e values shown in Refs. 23, 24. As one can see by looking at the figure, the spectrum obtained using a CCD more efficient in the NIR (dashed line) is closer to the spectrum obtained considering an ideal detector with respect to a detector optimized for the visible (dot-dashed). The dip between 500 and 600 nm is caused by hemoglobin absorption.

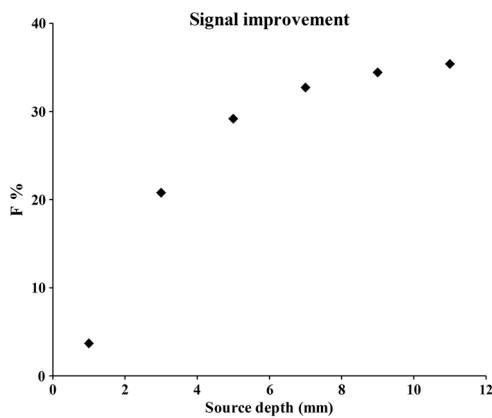


Fig. 2 The plot shows the figure of merit F calculated at different source depths, as one can see the figure of merit presents a monotonic increase with respect to source depth. This clearly shows that a detector optimized for the NIR always allows a better detection of the Cerenkov radiation exiting the animal tissues.

looking at Fig. 1, the spectrum obtained using a CCD more efficient in the NIR region is closer to the spectrum obtained considering an ideal detector.

F was calculated at different source depths ranging from 1 to 11 mm and plotted in Fig. 2. The plot presents a monotonic increase of F with respect to source depth, showing that a CCD optimized for the NIR always allows a better detection of the Cerenkov radiation exiting the animal tissues.

Considering only the Poisson nature of the noise, the relative differences in the signal to noise ratio (SNR) are $\approx(\sqrt{F+1}-1)$. For example, a value of $F = 35\%$ corresponds to a 16% improvement of the SNR.

Of course there are other important sources of noise like the CCD reading noise and dark current. These sources of noise are dependent on the detector temperature, electronics, and reading mode. A detailed analysis of all these noise sources is beyond the main goals of this short note.

The theoretical analysis presented here shows that the use of a CCD optimized for the NIR allows a better detection of the Cerenkov photons exiting the animal surface, suggesting that small animal optical imaging systems tailored on the NIR range perform well for CLI.

We would like to stress that our analysis is based on several assumptions and approximations like considering almost constant the particle speed and Cerenkov radiation emitted by a point source. However, we believe that these are not severe limiting factors. More precisely, our main goal was to compare in relative terms [see Eq. (12)] the efficiency of Cerenkov photons detection in the visible and NIR region and not to obtain absolute signal quantitation. The comparison was performed considering Cerenkov point sources located at different depths inside the animal.

We conclude that noninvasive CLI imaging can be improved by using small animal optical imaging systems based on a CCD detector with a quantum efficiency peaked in the NIR range. The improvement is more significant when the Cerenkov source to be imaged is located deeper inside the animal.

References

1. R. Robertson et al., "Optical imaging of Cerenkov light generation from positron-emitting radiotracers," *Phys. Med. Biol.* **54**(16), N355–N365 (2009).
2. A. E. Spinelli et al., "Cerenkov radiation allows *in vivo* optical imaging of positron emitting radiotracers," *Phys. Med. Biol.* **55**(2), 483–495 (2010).
3. A. E. Spinelli et al., "Cerenkov radiation imaging of beta emitters: *in vitro* and *in vivo* results," *Nucl. Instrum. Meth. A* **648**(Suppl. 1), S310–S312 (2011).
4. F. Boschi et al., "*In vivo* (18)F-FDG tumour uptake measurements in small animals using Cerenkov radiation," *Eur. J. Nucl. Med.* **38**(1), 120–127 (2011).
5. H. Liu et al., "Molecular optical imaging with radioactive probes," *PLoS One* **5**(3), e9470 (2010).
6. A. Ruggiero et al., "Cerenkov luminescence imaging of medical isotopes," *J. Nucl. Med.* **51**(7), 1123–1130 (2010).
7. A. E. Spinelli and F. Boschi, "Unsupervised analysis of small animal dynamic Cerenkov luminescence imaging," *J. Biomed. Opt.* **16**(12), 12 (2011).
8. H. Liu et al., "Radiation-luminescence-excited quantum dots for *in vivo* multiplexed optical imaging," *Small* **6**(6), 1087–1091 (2010).
9. R. S. Dohager et al., "Cerenkov radiation energy transfer (CRET) imaging: a novel method for optical imaging of PET isotopes in biological systems," *PLoS One* **5**(10), e13300 (2010).
10. M. A. Lewis et al., "On the potential for molecular imaging with Cerenkov luminescence," *Opt. Lett.* **35**(23), 3889–3891 (2010).
11. C. Ran et al., "*In vivo* photoactivation without 'light': use of Cerenkov radiation to overcome the penetration limit of light," *Mol. Imag. Biol.* **14**(2), 156–162 (2012).
12. C. Li, G. C. Mitchell, and S. R. Cherry, "Cerenkov luminescence tomography for small-animal imaging," *Opt. Lett.* **35**(7), 1109–1111 (2010).
13. Z. Hu et al., "Experimental Cerenkov luminescence tomography of the mouse model with SPECT imaging validation," *Opt. Express* **18**(24), 24441–24450 (2010).
14. A. E. Spinelli et al., "Multispectral Cerenkov luminescence tomography for small animal optical imaging," *Opt. Express* **19**(13), 12605–12618 (2011).
15. J. V. Jelley, *Cerenkov Radiation and Its Applications*, Pergamon, London (1958).
16. A. Zheltikov and K. Anokhin, "Fiber-probe detection for positron-emission-assisted Cerenkov-radiation brain mapping," *Phys. Rev. E* **6**, 061902–061907 (2011).
17. R. C. Haskell et al., "Boundary conditions for the diffusion equation in radiative transfer," *J. Opt. Soc. Am. A* **11**(10), 2727–2741 (1994).
18. B. W. Rice, M. D. Cable, and M. B. Nelson, "*In vivo* imaging of light-emitting probes," *J. Biomed. Opt.* **6**(4), 432–440 (2001).
19. P. A. Cerenkov, *Radiation of Particles Moving at a Velocity Exceeding That of Light, and Some of the Possibilities for Their Use in Experimental Physics, Nobel Lectures, Physics*, Elsevier Publishing, Amsterdam, 1942–1962 (1964).
20. G. S. Mitchell et al., "*In vivo* Cerenkov luminescence imaging: a new tool for molecular imaging," *Phil. Trans. A Math. Phys. Eng. Sci.* **369** (1955), 4605–4619 (2011).
21. C. Kuo et al., "Three-dimensional reconstruction of *in vivo* bioluminescent sources based on multispectral imaging," *J. Biomed. Opt.* **12**(2), 024007 (2007).
22. Living Image 4.0, Caliper Life Sciences, <http://www.caliperls.com/products/preclinical-imaging/living-image.htm> (last accessed 20 Feb 2011).
23. <http://www.caliperls.com/products/preclinical-imaging/ivis-imaging-system-200-series.htm> (last accessed 20 Feb 2011).
24. http://www.andor.com/pdfs/literature/Andor_iKon-M_Flyer.pdf (last accessed 20 Feb 2011).